The Journal of Experimental Biology 203, 3397–3409 (2000)
Printed in Great Britain © The Company of Biologists Limited 2000
JEB3053

THE OPTOMOTOR RESPONSE AND SPATIAL RESOLUTION OF THE VISUAL SYSTEM IN MALE *XENOS VESPARUM* (STREPSIPTERA)

WALTRAUD PIX[1,2], JOHANNES M. ZANKER[2] AND JOCHEN ZEIL[2,*]

[1]*Lehrstuhl für Biokybernetik, Universität Tübingen, Auf der Morgenstelle 28, D-72076 Tübingen, Germany* and [2]*Centre for Visual Sciences, Research School of Biological Sciences, Australian National University, PO Box 475, Canberra, ACT 2601, Australia*

*Author for correspondence (e-mail: zeil@rsbs.anu.edu.au)

Accepted 4 September; published on WWW 24 October 2000

Summary

The Strepsiptera are an enigmatic group of parasitic insects whose phylogenetic relationships are hotly debated. Male Strepsiptera have very unusual compound eyes, in which each of a small number of ommatidia possesses a retina of at least 60 retinula cells. We analysed the optomotor response of *Xenos vesparum* males to determine whether spatial resolution in these eyes is limited by the interommatidial angle or by the higher resolution potentially provided by the extended array of retinula cells within each ommatidium. We find that the optomotor response in Strepsiptera has a typical bandpass characteristic in the temporal domain, with a temporal frequency optimum at 1–3 Hz. As a function of spatial wavelength, the optomotor response is zero at grating periods below 12° and reaches its maximum strength at grating periods between 60° and 70°. To identify the combination of interommatidial angles and angular sensitivity functions that would generate such a spatial characteristic, we used motion detection theory to model the spatial tuning function of the strepsipteran optomotor response. We found the best correspondence between the measured response profile and theoretical prediction for an irregular array of sampling distances spaced around 9° (half the estimated interommatidial angle) and an angular sensitivity function of approximately 50°, which corresponds to the angular extent of the retina we estimated at the centre of curvature of the lens. Our behavioural data strongly suggest that, at least for the optomotor response, the resolution of the strepsipteran compound eye is limited by the ommatidial sampling array and not by the array of retinula cells within each ommatidium. We discuss the significance of these results in relation to the functional organisation of strepsipteran compound eyes, their evolution and the role of vision in these insects.

Key words: Strepsiptera, *Xenos vesparum*, eye, vision, optomotor response, resolution.

Introduction

Peculiar eyes

The optics of adult winged insects typically consists of three single-lens ocelli grouped together on the vertex of the head and a pair of large lateral compound eyes. The compound eyes, each of which contains several thousand closely packed ommatidia, are well suited for visual tasks, such as object or motion detection, that require or profit from a good spatial resolution. Compared with this typical design, the compound eyes of male Strepsiptera are extremely peculiar (Fig. 1A). Each of the hemispherical eyes is composed of only a few ommatidia (20–50 in most species) with as few as 10 in *Tridactylophagus similis* and as many as 150 ommatidia in *Stylops muelleri* (Kinzelbach, 1971). The large circular lenses are well separated from one another by heavily sclerotized and usually pilose cuticula. Their arrangement on the eye surface is irregular, their sizes vary significantly across the eye, and their numbers can differ between the left and the right eye in an individual animal (Kinzelbach, 1971).

In *Xenos vesparum*, the eyes have, on average, 65 ommatidia, although the numbers in the left and the right eye frequently differ by 10–15 (Kinzelbach, 1967). Beneath each of the strongly biconvex lenses, the microvilli of at least 60 retinula cells form an extended reticular and vertically layered (tiered) rhabdom structure (Fig. 1B–D; Strohm, 1910; Rösch, 1913; Wachmann, 1972). The eyes of male Strepsiptera have been considered to be modified larval compound eyes because of their appearance in early larval stages and the arrangement of photoreceptors, which resembles that found in stemmata, the single-lens eyes of holometabolous larvae (Kinzelbach, 1971; Paulus, 1979). Compound eyes in adult insects with a small number of dispersed ommatidia are confined to the originally wingless insects Collembola and Zygentoma (Paulus, 1979) and

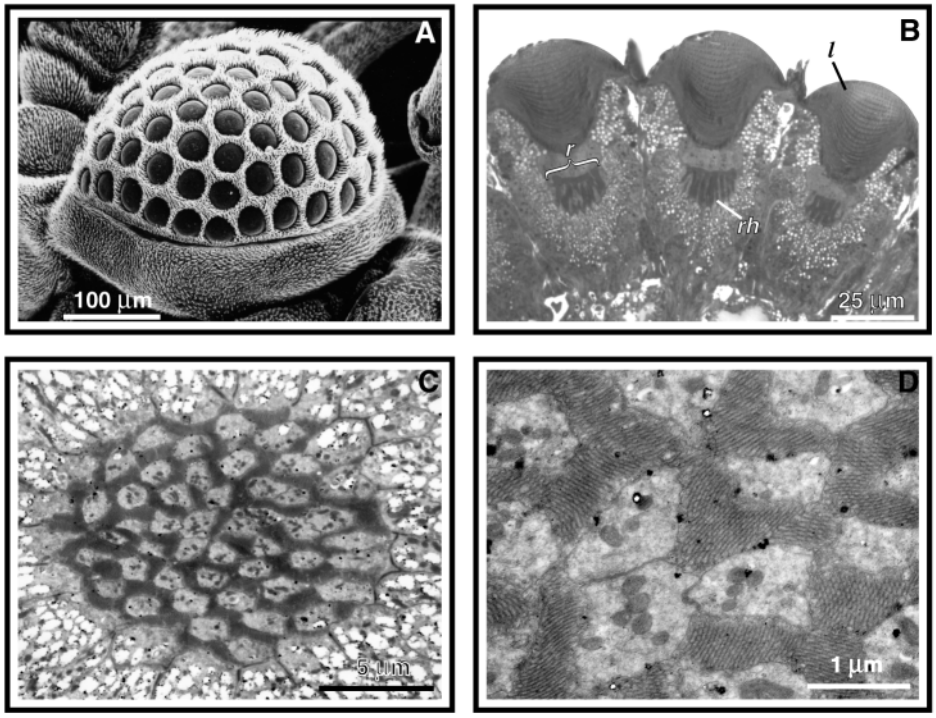

Fig. 1. (A) The eye of a male *Xenos vesparum*, in a fronto-ventral scanning electron micrograph. (B) Vertical semi-thin section through a set of ommatidia showing the biconvex lens (*l*) and the flat retina (*r*) with a palisade of rhabdoms (*rh*). (C) Electron micrograph of a horizontal section through the distal retina showing the network of rhabdomeres. The vacuolated compartments around the retina contained screening pigment that was removed by treating the preparation with NaOH after the first fixation with glutaraldehyde. (D) Electron micrograph of a horizontal section through part of the rhabdom at higher magnification.

peculiarly to the males of primitive scale insects (Jancke, 1955). It has been suggested that strepsipteran eyes model for the schizochroal eyes of the fossil phacopid trilobites, since the external morphology of the eyes in both groups exhibits striking similarities (Horváth et al., 1997).

So far, the functional and behavioural significance of the eye anatomy of male Strepsiptera is not understood. Strepsiptera are highly specialized parasites of other insects. Most of their unique characteristics are considered to be related to their parasitic life style. With the exception of the original Mengenillidae, the wingless females lack eyes and legs and stay resident in their insect hosts throughout their life. The agile males, in contrast, after emerging from the puparium, spend approximately 1 h of their short adult life on the wing searching for hosts that carry receptive females. The males are known to be attracted by female odour (Ulrich, 1956; Linsley and MacSwain, 1957). It is unclear whether vision is involved in mating behaviour. The study of functional aspects in Strepsiptera is hampered by the fact that collecting and handling these tiny, short-lived and delicate animals is extremely difficult. The little we know about the visual capabilities of male Strepsiptera stems from a behavioural study aimed primarily at elucidating the function of the modified forewings of male *Xenos vesparum*, which look and function like the halteres of dipteran flies (Pix et al., 1993). The results of that study suggested that Strepsiptera males use both visual and mechanical cues to compensate for involuntary rotations in flight. Moving a patterned cylinder around the animals elicits compensatory head and abdomen movements, indicating that Strepsiptera males exhibit a ‘classic’ optomotor response.

Behavioural analysis of the optical transfer properties in compound eyes

The aim of the present study was to investigate the functional characteristics of strepsipteran compound eyes, not least because a recent account advances the hypothesis that image resolution in these eyes is limited by the retinal sampling array (Buschbeck et al., 1999). Given their unusual anatomy and their uncertain phylogenetic status (e.g. Crowson, 1981; Kathirithamby, 1989; Kinzelbach, 1990), it is of particular interest to know whether the spatial resolution of the eyes is limited by the ommatidial sampling distance or by a sampling distance based on the angular separation of receptor subunits within the retina of a single ommatidium. To this end, we determined the temporal and spatial frequency characteristics of the strepsipteran optomotor response.

Optomotor responses are highly stereotyped behavioural responses driven by image motion information, which is extracted from the image flow at the retina during self-motion. Flying insects respond to involuntary changes in their body posture with various flight steering manoeuvres such as changes in the wingbeat or abdomen deflections that tend to keep body orientation constant in the presence of disturbances (Götz et al., 1979; Zanker, 1988). In addition, the insects turn their head to minimise image shifts across the retina (for a review, see Hengstenberg, 1993). These compensatory responses can be elicited experimentally by moving patterns around tethered flying animals.

Since the significance of our results relies heavily on a detailed understanding of the principles of motion detection underlying the optomotor response, we briefly summarize what is known about the optomotor response and how it is

influenced by the optical design of the compound eye. In insects, image motion is computed from spatially correlated changes in light intensity at the retina. On the basis of extensive stimulus/response analyses in beetles and flies, it has been proposed that the elementary mechanism underlying motion detection involves a correlation between signal changes in neighbouring inputs (for reviews, see Borst and Egelhaaf, 1989, 1993). An elementary motion detector (EMD) consists of two spatially separated input elements, two temporal filters, two multiplication units and a subtraction stage. A moving stimulus activates two input channels one after the other. By delaying the signal of the channel that has been stimulated first by an appropriate time interval (employing a delay or low-pass filter), the input signals eventually coincide at the stage at which they are multiplied by each other. The result of this interaction is a large signal from the EMD output whenever the movement has the appropriate speed and is in the 'preferred' direction of the detector. When the stimulus moves in the opposite direction, the temporal separation of the signals is increased at the multiplication stage, and the result is only a small output signal. The motion detection underlying the optomotor response operates on the spatial and temporal distribution of light intensity that is represented on an array of input elements (e.g. receptors) feeding into an array of EMDs.

The structure of EMDs allows one to predict several aspects of behavioural reactions to wide-field image motion. First, regardless of the particular type of EMD, the limit of spatial resolution depends only on the sampling base $\Delta\phi$ of the EMDs, given by the angular separation of its two input elements, and on the width of the angular sensitivity function of the input elements, $\Delta\rho$. These two variables determine how the response of the EMD depends on the spatial properties of a moving pattern. Second, for moving sinusoidal gratings, the response peaks at a given temporal frequency, irrespective of the spatial wavelength of the pattern. The velocity optimum of the response is related to the sampling base and the time constant of the temporal filter. As the spatial wavelength of the moving pattern increases, the response optimum of an EMD shifts towards higher velocities in such a way that the ratio of the most efficient velocity to the spatial wavelength of a pattern (the temporal frequency) remains constant. If the temporal frequency is kept constant, while the spatial wavelength, λ, is varied, the response has a maximum when $\lambda=4\Delta\phi$.

The sampling base of the detector therefore limits the range of resolvable spatial frequencies. According to the sampling theorem of Shannon (Shannon and Weaver, 1949), the smallest spatial wavelength of a moving pattern that can be reliably transmitted by an array of input elements is equal to twice the sampling base of the detector. Finer gratings evoke an apparent reversal of the direction of pattern motion. This phenomenon, known as spatial aliasing, is based on geometrical interference between the moving grating and the sampling array of the input elements (von Gavel, 1939; Hassenstein, 1951; Götz, 1964). A maximum response is expected when the spatial wavelength is four times the sampling base; with larger wavelengths, the response to moving patterns decreases again. Aliasing errors caused by undersampling are reduced by the spatial filter properties of the input elements. In compound eyes, the input elements are either the photoreceptors in neighbouring ommatidia, as in the case of eyes with fused rhabdoms, or the photoreceptors within one ommatidium, as in the case of eyes with open rhabdoms. The half-width of the bell-shaped angular sensitivity function of the receptor or rhabdom, $\Delta\rho$, determines the spatial cut-off frequency, i.e. the highest spatial frequency that can be transmitted with some detectable contrast by the optical system. In most day-active insects, the ratio between the angular sensitivity function of receptors and the angular separation of optical axes of neighbouring ommatidia or receptors ranges between 0.5 and 2 (Götz, 1965; Warrant and McIntyre, 1993; Land, 1997) whereby the optimal sampling strategy demands that $\Delta\rho/\Delta\phi=2$.

Our attempt to determine whether the resolving power of the strepsipteran eye depends on the angular separation of the ommatidia or on a much smaller sampling base provided by the individual rhabdomeres of the retinula cells within individual ommatidia will be covered in several steps. First, we describe qualitatively the optomotor response to moving stimulus gratings in *Xenos vesparum*. Second, we present a quantitative analysis of the behavioural response to pattern motion while systematically varying spatial and temporal stimulus variables to determine the limits of the spatial resolution of the strepsipteran eye. Third, we compare the experimental results with the response of an EMD model, which allows us to identify the sampling base and the angular sensitivity function of the input stages of those EMDs that contribute to the optomotor response. We then compare our results with anatomical estimates of interommatidial angles, inter-receptor angles and angular sensitivity functions, and we discuss their significance for a functional interpretation of strepsipteran compound eyes.

Materials and methods

Polistes dominulus Linnaeus (Vespidae, Hymenoptera) infected by *Xenos vesparum* Rossi males were collected from the end of July to the beginning of August in the vicinity of Tübingen, South Germany, and kept individually in small containers in a dark place. The *X. vesparum* males were induced to emerge by placing small groups of 3–5 hosts under a bright mercury vapour lamp or in a sunny place. During the light exposure, the wasps were carefully observed, and emerging *X. vesparum* males were immediately separated from their hosts, immobilized by cooling in a refrigerator and waxed with the ventral or the dorsal side of their metathorax to a piece of wire. They were then centred inside a cylinder (diameter 14.5 cm) that could be rotated at a range of speeds with the aid of a servomotor and which could be fitted with different patterns. The square patterns used for visual stimulation consisted of 15 cm long vertical black-and-white stripes of identical width with spatial wavelengths ranging from 5.6 ° to 180 ° (64–2 cycles in the cylinder).

The patterns were illuminated by a circular ring light source

mounted above the pattern cylinder. The animals were filmed through the ring light source from above with a Panasonic F10 CCD video camera (25 fields s^{-1}), equipped with a Panagor 90 mm macro lens and extension tubes, providing a video image that covered an area of approximately 0.4 cm×0.54 cm. The large magnification necessary to record the head and abdomen movements of these tiny animals, which have a body length of approximately 0.35 cm, made it impossible to record the pattern directly on the video image. The movement of the pattern was therefore determined by recording the orientation of a blurred image of a thin thread across the cylinder. Control experiments excluded the possibility that the moving thread on its own elicited visual responses. Alternatively, a signal proportional to the rotational velocity of the patterned cylinder was electronically added to the video image, using the signal from the control unit for the servomotor that drove the cylinder.

The *X. vesparum* males were oriented inside the patterned cylinder such that the pattern was rotated around the yaw axis of the animal. Head and abdomen movements in response to pattern rotations were determined frame by frame from digitised video images. The angular position of the head with respect to the body in the horizontal plane was determined by the angle of a line connecting the most lateral parts of the left and right eyes, representing the transverse axis of the head, and a line between the anterior tip of the metathoracic scutum and the posterior tip of the pronotum, indicating the longitudinal axis of the body. The angular position of the abdomen with respect to the body was determined by the angle between the longitudinal axis of the body and a line connecting the posterior tip of the pronotum and the tip of the abdomen. A deflection of the head or of the abdomen with respect to the longitudinal axis of the body in a counter-clockwise direction was defined as positive.

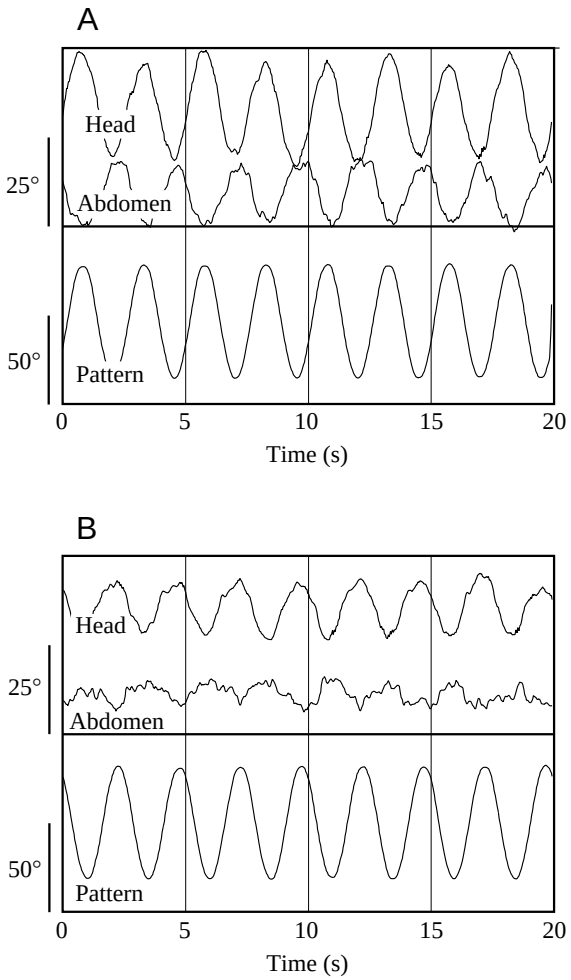

Fig. 2. Compensatory head and abdomen movements around the yaw axis of a *Xenos vesparum* individual in response to oscillating gratings with a spatial wavelength λ (A) of 60° and (B) of 45°. The time courses of the angular position of the head (top) and of the abdomen (centre) are shown relative to the longitudinal axis of the body. The sampling interval was 40 ms, and the traces were smoothed with a three-point weighted filter. The bottom trace shows the angular position of the pattern (note the different scales for the stimulus and response traces). The pattern in both A and B oscillated around the yaw axis of the animal at a temporal frequency of 0.4 Hz with a peak-to-peak amplitude of 64°. Pattern rotation evokes head-following movements and abdominal deflections in the opposite direction. The head movements reduce the retinal slip speed directly, whereas the abdominal response probably elicits corrective steering manoeuvres during free flight.

Results

The optomotor response in male Xenos vesparum

X. vesparum males respond to a moving pattern around the yaw axis with characteristic postural changes. The shift in the image on the retina of the animal simulates a free-flight situation in which the animal experiences a body yaw in a static environment. When the pattern is oscillated sinusoidally, the head appears to follow the pattern movement in regular cycles, and the abdomen is deflected in the opposite direction to that of the pattern motion (Fig. 2). We calculated the head response gain as the ratio of the peak-to-peak amplitudes of the head and pattern oscillations. For the pattern with a spatial wavelength of λ=60° (Fig. 2A), this gain is approximately 0.45, which is approximately twice the size of that elicited by the pattern with λ=45° (Fig. 2B). Under these experimental conditions, the animal therefore compensates for less than half of the retinal image shift. However, in free flight, the response of the head to the mechanosensory perception of a real body rotation mediated by the forewings would further reduce the slip speed, at least in the range of high angular speeds (Pix et al., 1993). Furthermore, the head response will be accompanied by flight-steering movements such as the abdominal deflection (see Fig. 2). During free flight, these deflections result in the correction of involuntary changes in the body orientation, as proposed for the abdominal deflections of flies in similar situations (Götz et al., 1979; Zanker, 1988). Again, the amplitude of the abdominal movement elicited by rotating the pattern with the larger wavelength, λ=60°, is roughly twice that elicited by the λ=45° pattern motion.

To determine the dependence of the optomotor response on

the spatial and temporal properties of the stimulus, we measured the response elicited by patterns of constant spatial wavelength moving at different angular velocities and then repeated the measurements with patterns of different spatial wavelengths. Fig. 3 shows the response of an individual animal to a sequence of changes in motion direction (Fig. 3A) and the way in which we calculated the mean response amplitude to a single velocity step (Fig. 3B). The pattern of black-and-white vertical stripes with a spatial wavelength of 45 ° was rotated at a constant velocity of 100 ° s^{-1}, alternating between a clockwise and a counter-clockwise direction. The pattern rotation lasted at least 5 s, and the clockwise and counter-clockwise rotations were separated by intervals of 0.5–1 s, during which the pattern remained still. The *X. vesparum* male moves its head in the direction of the pattern movement, and approximately 1.5 s after stimulus onset the head deflection approaches a plateau, which is more-or-less maintained until the motion stops. After the cessation of the stimulus and during the short periods without motion stimulation, the head slowly moves back towards an intermediate (zero) position. Values of the mean head response amplitudes were obtained in the following way. Data were collected during the plateau phase of the response 2 s after stimulus onset. For each clockwise and counter-clockwise pattern rotation, we took five measurements at consecutive 200 ms time intervals. The mean response amplitudes were determined by taking measurements at each stimulus direction for three cycles. Their difference divided by 2 was plotted with the standard errors of the mean, as if the pattern had been moving only counter-clockwise.

Compared with the deflection of the head, the response of the abdomen to the pattern movement is less regular. After an initial deflection in response to stimulus onset, the orientation of the abdomen fluctuates considerably (Fig. 3A). These spontaneous movements sometimes include up- and downward deflections, which made it difficult to detect the abdomen tip reliably. We therefore restricted the analysis of the optomotor response to the head reflexes.

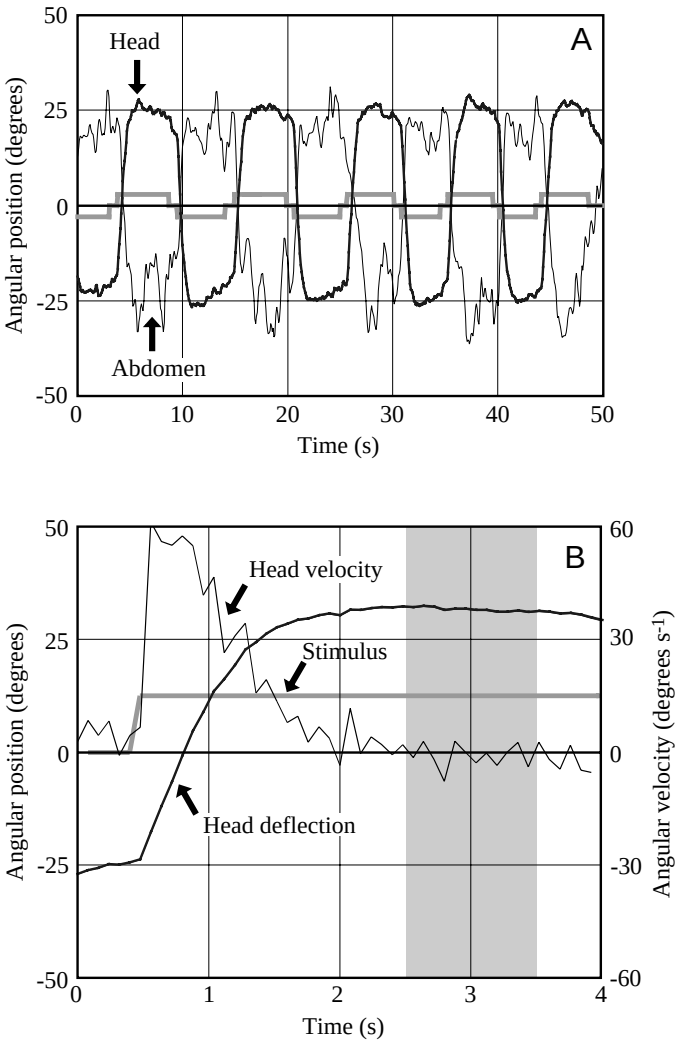

Fig. 3. Optomotor responses of an individual male *Xenos vesparum* elicited by pattern movement at constant speed, alternating between a clockwise (negative) and a counter-clockwise direction (positive). (A) The angular position of the head (thick line) and abdomen (thin line) relative to the longitudinal body axis in the horizontal plane are plotted as a function of time. The dark grey line with a rectangular time course shows the intervals during which the pattern was in motion, and its sign (spatial wavelength λ=45 °, angular velocity v=100 ° s^{-1}). The sampling interval was 80 ms, and traces were smoothed with a three-point weighted filter. (B) Averaged head response during the first few seconds after stimulus onset. The time course of the head deflection (thick line; left-hand scale) and the angular velocity of the head (thin line; right-hand scale) obtained from the data in A. The sign of the head response to clockwise stimulation has been inverted. Approximately 1.5 s after stimulus onset, the head response approaches a plateau and the velocity has declined to zero. The grey-shaded area indicates the time interval during which samples were taken to measure the mean amplitude of the head response.

Stability of the behaviour

One difficulty with quantitatively analysing the optomotor response in Strepsiptera males was the change in responsiveness in individual animals during an experimental session. *X. vesparum* males live for only a few hours. In the laboratory, the flight activity of freely flying animals did not exceed 1.5 h and in most cases it lasted considerably less. When glued to a holder, flying *X. vesparum* males often respond only weakly and sometimes not at all to visual stimulation, although they flap their wings with full amplitude. In cases in which the animals initially responded reliably to pattern motion, the responses diminished within an hour of starting the experiments. We therefore used a standard visual control stimulus interspersed among experimental blocks to monitor the overall response state of the animals. To compare data from different experimental blocks, we rejected all measurements whenever the response elicited by the control stimulus was less then 80 % of the maximum response to this stimulus. Fig. 4 shows an example of how the behavioural responses were evaluated by using a control stimulus.

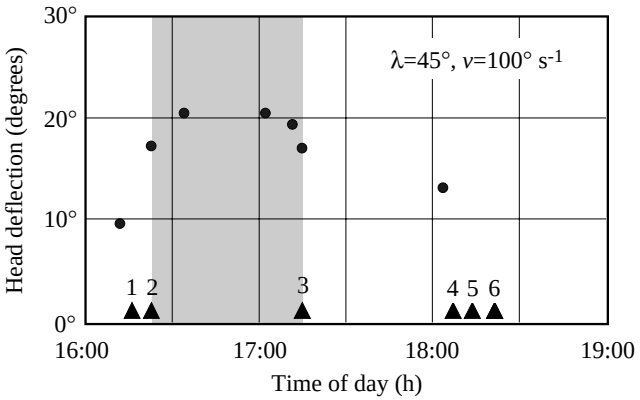

Fig. 4. The optomotor response profile of a male *Xenos vesparum* during a complete experimental session. The mean amplitudes of head deflections in the horizontal plane are plotted as a function of the time of day. The filled circles indicate the mean amplitudes of the head response elicited by a control stimulus, consisting of a pattern of black-and-white stripes with a spatial wavelength λ of 45° moving at a constant velocity *v* of 100° s^{-1}. The control stimulus was presented at irregular times between different experimental blocks to monitor the overall response of the animal. The only data considered for further analysis were those collected during a time period, indicated by the grey-shaded area, in which the amplitude of the response to the control stimulus was equal to or larger than 80% of the maximum response (20.5° in this example). The triangles and numbers on the abscissa indicate the following events: (1) start of continuous flight; (2) start and (3) end of the interval used for experimental analysis; (4) onset of irregular flight (irregular pitch movements of the thorax and short cessations of hindwing movements); (5) start of intermittent flight (frequent cessations of both fore- and hindwing movements); (6) cessation of flight.

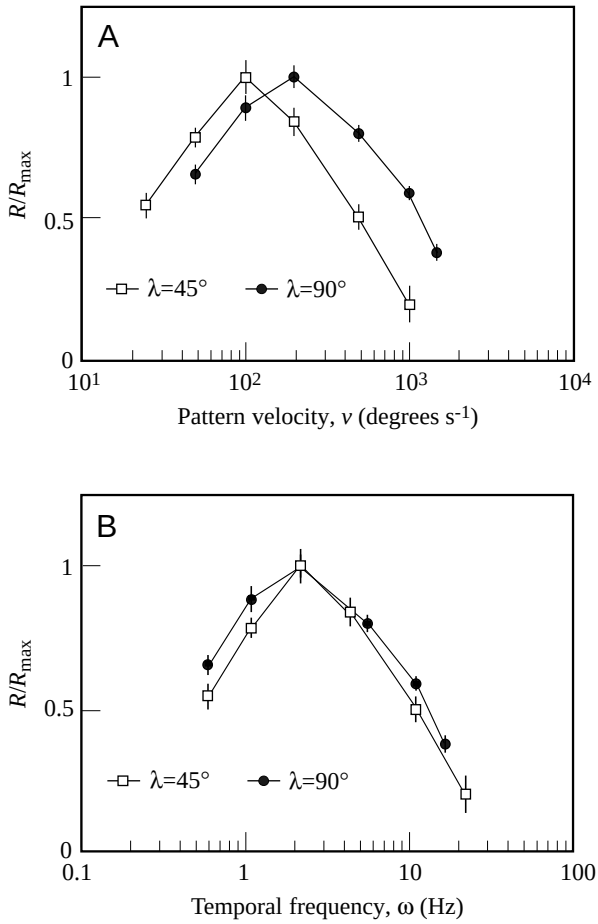

Fig. 5. Dependence of the optomotor response on the velocity and the spatial wavelength of a moving pattern. Mean response amplitudes (*R*) for patterns with wavelengths λ of 45° and 90° are plotted against pattern velocity (*v*) (A) and against the temporal frequency (ω) (B). Response amplitudes have been normalised to maximum (R_{max}). Data are from two animals, one was stimulated with the 45° pattern, the other with the 90° pattern. Values are means ± S.E.M., *N*=6.

Dependence of the optomotor response on the spatial frequency of the stimulus

As we have outlined in the Introduction, the optomotor response can be used to determine the spatial organisation of the motion detector input elements by comparing it with predictions made by the theory of correlation-based mechanisms for motion detection. A characteristic property of correlation-type motion detectors, which has been extensively studied in flies, is the dependence of their output on the temporal frequency of a periodic stimulus, i.e. the ratio of the angular velocity *v* (degrees s^{-1}) to the spatial wavelength λ (degrees) of a moving grating, rather then on *v* alone (see below for more details). The direction of grating displacement can be correctly resolved only by an array of detector input elements if the period λ of the grating is larger than twice the separation of the input elements Δφ. The 'resolution limit', as obtained from the optomotor response, can therefore be used to determine the functional interommatidial angle in the strepsipteran eye and, as we will see below, also the angular sensitivity function of the input units, which normally consist of individual receptor cells in insects.

Fig. 5 shows an example of how the optomotor response in *X. vesparum* males depends on the angular velocity *v* and spatial wavelength λ of the stimulus pattern. The data are from two animals responding to moving patterns with λ=45° and λ=90° and angular velocities ranging over approximately 2 log units (12.5 to 1600° s^{-1}). The response amplitudes increase with increasing pattern speed until they reach a maximum and decrease again at higher angular velocities (Fig. 5A). The response curves show a similar shape for the two different wavelengths, but the maxima appear at different angular velocities in such a way that the responses peak at the same temporal frequency of the stimulus, at $v/\lambda \approx 2.2$ Hz (Fig. 5B). The response therefore depends on the temporal frequency, $\omega = v/\lambda$, of the stimulus rather than on the speed of the pattern. This property of the optomotor response in *X. vesparum* provides strong evidence that the underlying motion-detection mechanism involves correlation-type detectors (Borst and Egelhaaf, 1989).

We measured the optomotor response in a number of

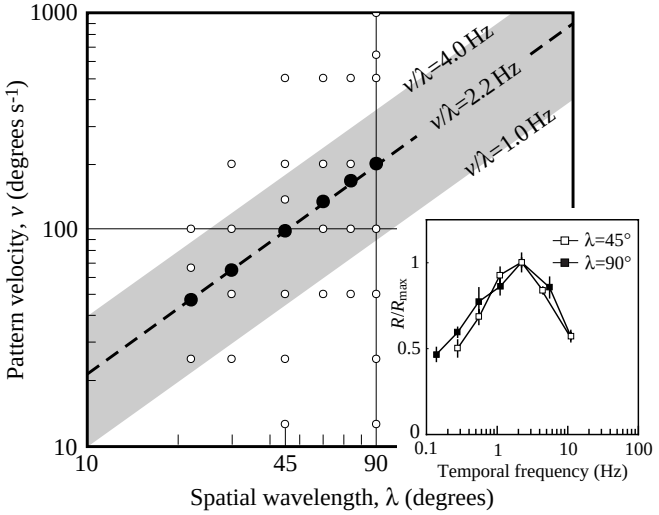

Fig. 6. The combinations of spatial wavelengths and rotational speeds of a moving periodic pattern at which the optomotor response was measured. The inset shows the response of one animal at pattern wavelengths λ of 45° and 90°. The response amplitude R has been normalised to R_{max}. Values are means ± S.E.M., N=6. The shaded area encloses temporal frequency values between 1 and 4 Hz, where the response optimum is likely to be found (see Fig. 5B and inset). Filled circles mark those combinations for which the response was at its maximum; open circles mark all the other stimulus combinations tested (see inset). The response optima are located on a straight line with a slope of v/λ=2.2 Hz, where v is pattern velocity, which indicates that the response is determined by the temporal frequency of the stimulus and that 2.2 Hz is close to the optimal temporal frequency for all the animals tested. Number of animals: λ=45°, three; λ=90°, four; at all other λ values, one. For details, see text.

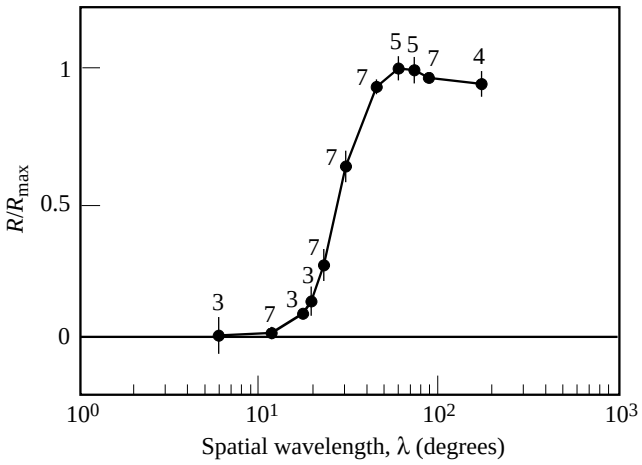

Fig. 7. Dependence of the optomotor response (R) on the spatial wavelength (λ) of the stimulus pattern. The mean amplitudes of the head response normalised to R_{max} (filled circles) and standard errors of the mean are shown as a function of λ at a constant temporal frequency ω=2.2 Hz of the stimulus. Numbers indicate the number of animals from which data were collected.

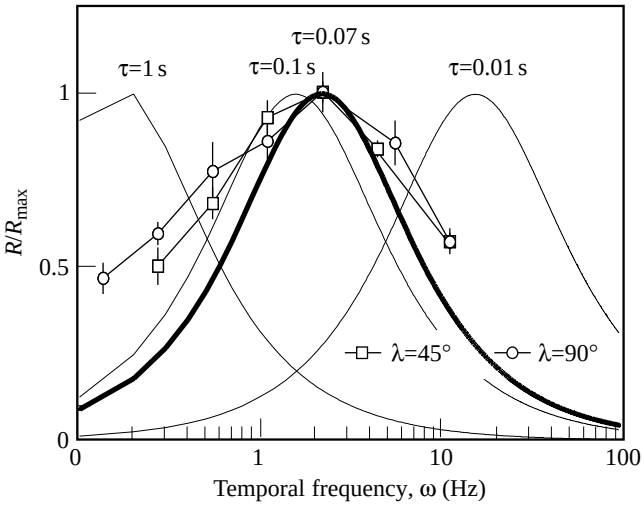

Fig. 8. Elementary motion detector response (R), normalised to R_{max}, as a function of the temporal frequency (ω). The location of the response maximum depends on the time constant τ. The optimum of the optomotor response in *Xenos vesparum* is at 2.2 Hz (data points from inset in Fig. 6) and corresponds to a time constant of approximately 0.07 s (thick line).

animals as a function of the pattern speed for different spatial wavelengths in the range between λ=22.5° and λ=90°. The combination of values we chose to test is shown as filled and open circles in Fig. 6, in which angular velocity is plotted as a function of wavelength. We knew from measurements of the type shown in Fig. 5 that the temporal frequency optimum of the optomotor response lies between 1 and 4 Hz, and we therefore chose combinations of spatial wavelengths and pattern velocities that would generate temporal frequencies within this range (shaded area in Fig. 6). We included a series of combinations with a temporal frequency of 2.2 Hz, and these always elicited a maximal response (filled circles, dashed line in Fig. 6). Examples of the response profiles for one animal at spatial wavelengths λ=45° and λ=90° are shown in the inset of Fig. 6.

We then determined the dependence of the optomotor response on the spatial wavelength of the stimulus pattern by combining each grating wavelength λ with the appropriate angular velocity v such that the temporal frequency of the stimulus was kept constant at ω≈2.2 Hz. As we have seen, the response is expected to be at the temporal frequency optimum for each wavelength under these experimental conditions. The response curve of the mean response amplitudes as function of λ shows maximal values between 40° and 80° (Fig. 7). No inversion of the response was found at shorter spatial wavelengths. This differs from the behavioural responses observed in other insects and from the responses predicted by a standard correlation model of motion detection (Götz, 1964). To interpret these experimental data, we compared the optomotor response properties determined in our behavioural experiments with the theoretical responses of elementary movement detectors (EMDs) of the correlation type. The comparison should reveal the sampling base and angular sensitivity functions of the EMD input elements, which

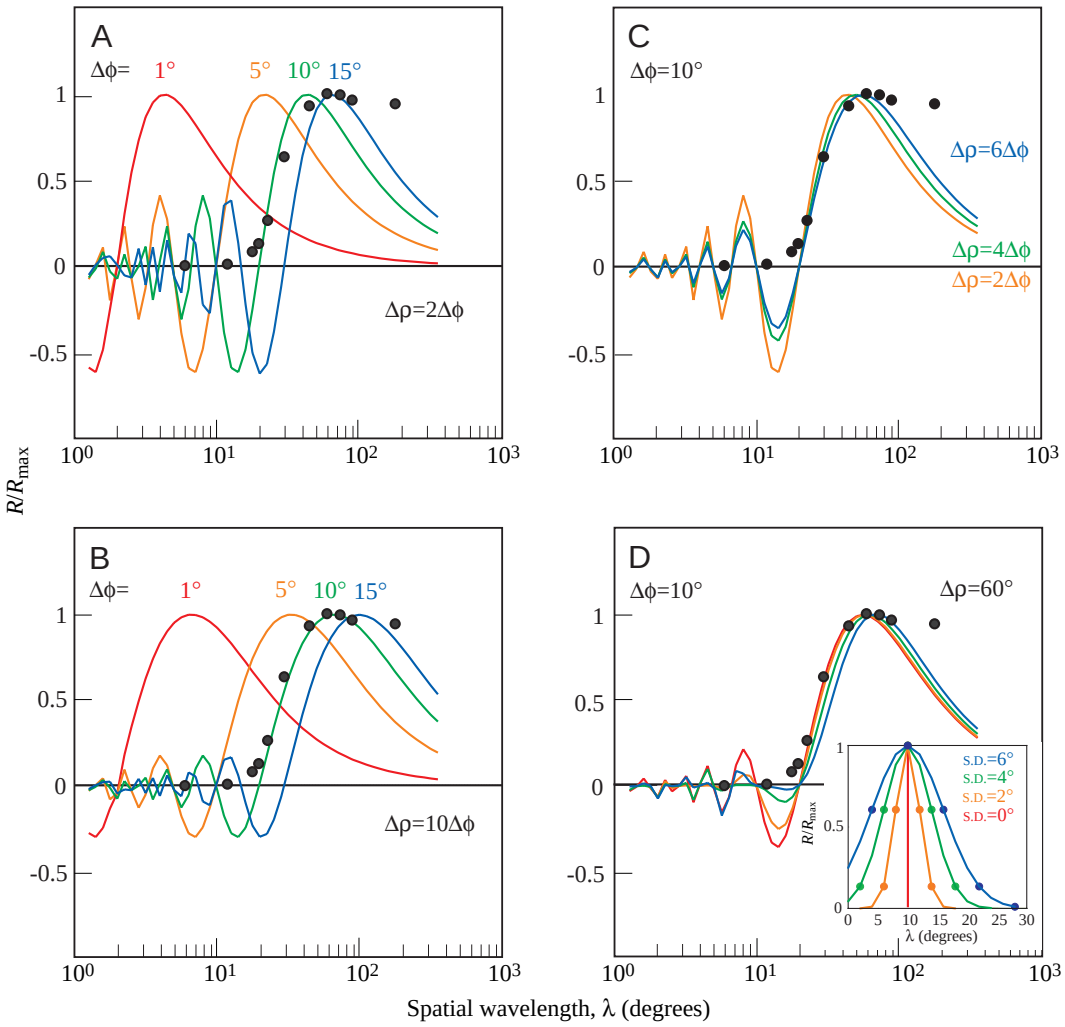

Fig. 9. Dependence of the elementary motion detector model response (R) on the spatial properties of the input elements. The model responses (coloured lines) are compared with the results of the behavioural experiments (filled circles, data from Fig. 7). The response amplitude R has been normalised to R_{max}. (A) Variation in the angular separation between the input elements, Δϕ, with the angular acceptance function Δρ=2Δϕ. (B) As in A, but with Δρ=10Δϕ. (C) The effects of varying Δρ. (D) Simulating the combined effects of irregularities and different sampling bases. The model responses were generated by adding the contributions of detectors with five different sampling bases (mean, ±1 S.D., ±2 S.D.). The contributions were weighted according to normal distributions with the same mean at 10°, but different standard deviations (see inset). For the blue model response, for instance, the values for sampling bases and their weights (in parentheses) are: Δϕ=10° (1.0), Δϕ=16° and 4° (0.607), Δϕ=22° (0.135), Δϕ=28° (0.011). The angular acceptance function Δρ was assumed to be constant at 60° (6Δϕ).

determine the resolution of the strepsipteran eye in the context of the optomotor response.

Modelling the properties of the optomotor response

The average steady-state response R of an EMD is a function of the angular velocity v and the spatial wavelength λ of the input pattern and of three detector variables, namely its time constant, τ, the angular separation of the input elements, Δϕ, and the width of the angular sensitivity function of the input elements, Δρ (Buchner, 1984; Reichardt, 1987) so that:

$$R \approx 1/\sqrt{[1+(2\pi\tau v/\lambda)^2]} \times \sin[\arctan(2\pi\tau v/\lambda)] \times \sin(2\pi\Delta\phi/\lambda) \times 1/\sqrt{[1+(\Delta\rho/\lambda)^2]}. \quad (1)$$

The term $1/\sqrt{[1+(2\pi\tau v/\lambda)^2]}$ is the amplitude factor of the first-order low-pass filter in the EMD, which depends on the number of luminance cycles that pass an input element per second, i.e. the temporal frequency, $\omega=v/\lambda$. The term $\sin[\arctan(2\pi\tau v/\lambda)]$ is often called the temporal frequency term, because it is responsible for the tuning of the detector to an optimal temporal frequency. The two temporal terms affect the average EMD response as a constant, as long as the time constant τ does not change and as long as care is taken to keep the temporal frequency ω constant in an experimental setting. Under these conditions, the average response is determined solely by the spatial properties of the pattern and of the sampling array and is independent of the properties of the temporal pattern. The response is then modulated by a sine function of the ratio of the sampling base Δϕ to the spatial wavelength λ of the periodic stimulus pattern. This so-called interference term, $\sin(2\pi\Delta\phi/\lambda)$, provides a quantitative prediction of the variation of the EMD response with λ. The largest response is expected for $\lambda=4\Delta\phi$, since the sine has a maximum at an angle of π/2. Patterns with wavelengths $\Delta\phi<\lambda<2\Delta\phi$, corresponding to the range between sinπ and sin2π, will invert the sign of the EMD response, which is referred to as spatial aliasing, or as geometric interference, between the periodic pattern and the EMD input array. Thus, the maximum, the zero-crossing and the minimum of the sine function can be used to evaluate the spatial organization of the EMD. The remaining term, $1/\sqrt{[1+(\Delta\rho/\lambda)2]}$, modulates the response in the manner of a spatial low-pass filter, depending

on the spatial frequency, $1/\lambda$, and the angular sensitivity function, $\Delta\rho$. Without this term, the maximum of the interference term and its minimum for the inversion at $\lambda=3\pi/2$ would have the same amplitude. This would only be the case, however, if the input elements had a needle-shaped angular sensitivity function, which would transmit arbitrarily small wavelengths without attenuation. Real photoreceptors, in contrast, have a broad angular sensitivity function because of the diffraction of light by the optical system and because of the finite acceptance angle of the rhabdoms (see Warrant and McIntyre, 1993). Within the angular sensitivity function of a receptor cell, periodic patterns with $\lambda<\Delta\rho$ are spatially pooled across more than one cycle and are therefore transferred with attenuated contrast. As a consequence, the response amplitude will be smaller in the range of high spatial frequencies than would be expected without the low-pass filter effects of the optics.

Let us first consider the temporal terms $1/\sqrt{[1+(2\pi\tau v/\lambda)2]}$ and $\sin[\arctan(2\pi\tau v/\lambda)]$ of the EMD. Together, the terms generate an output characteristic that resembles a symmetrical band-pass filter with a maximum amplitude at a specific temporal frequency, which depends on the size of the time constant τ (Fig. 8). If τ is very small (for instance $\tau=0.01$ s), the EMD responds to a large range of high temporal frequencies with an optimum at 15.9 Hz. With a large time constant ($\tau=1$ s), the EMD responds to a range of low temporal frequencies, with a response optimum at $\omega=v/\lambda=0.2$ Hz. We systematically varied τ until the response optimum corresponded to that for the optomotor response in *X. vesparum* at a temporal frequency of $\omega=2.2$ Hz for all spatial wavelengths λ (see Figs 5, 6). The result of this exercise is an estimate of τ of approximately 0.07 s (Fig. 8).

Since we kept the temporal frequency constant in the experiments that are relevant here (Fig. 7), we can be reasonably sure that the motion detector response of the insects was independent of the temporal pattern properties and was determined only by their spatial properties and those of the visual system. The response then represents a low-pass-filtered version of the geometric interaction between the sampling array and the periodic pattern. Unfortunately, we could not use the most straightforward measure, namely the inversion of the sign of the EMD response at spatial wavelengths in the range of $\Delta\phi<\lambda<2\Delta\phi$, which is predicted by the interference term in equation 1. As can be seen in Fig. 7, we did not find such an inversion of the optomotor response in *X. vesparum*, although the possibility remains that we may have missed one between $\lambda=5°$ and $\lambda=12°$ (but see below). In an attempt to explain this observation, we varied $\Delta\phi$ and $\Delta\rho$ in equation 1 to determine the range of values that would reproduce the particular characteristic of the measured optomotor response.

We first tested the effects of varying the angular separation $\Delta\phi$ of the input elements; $\Delta\phi$ corresponds either to the interommatidial angle or to the inter-receptor angle in the strepsipteran eye. We chose $\Delta\phi$ values of 1°, 5°, 10° and 15° and for the angular sensitivity function, $\Delta\rho$, values that were multiples of $\Delta\phi$. The model output was then compared with the

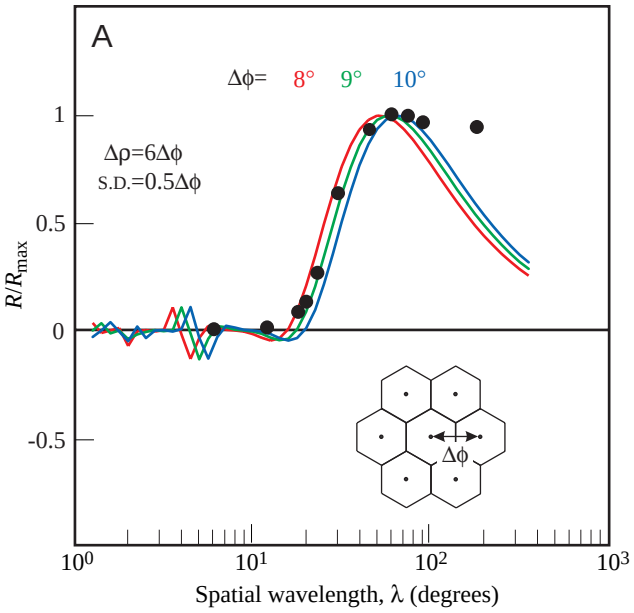

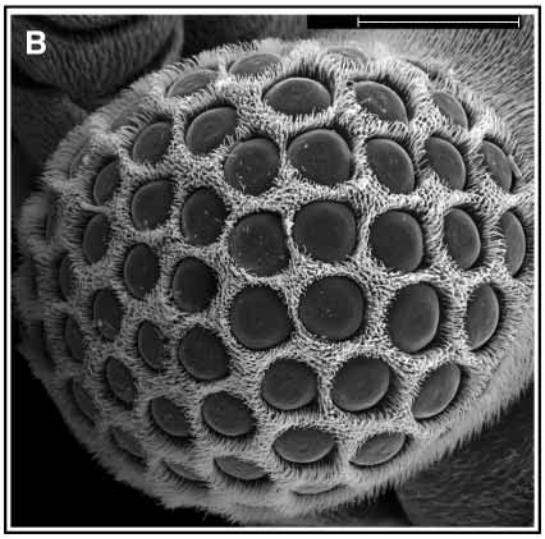

Fig. 10. (A) Experimental data and model responses (R) normalised to R_{max} for distributions of sampling bases around means of 8°, 9° and 10°, with standard deviations (S.D.) of 0.5$\Delta\phi$, and $\Delta\rho=6\Delta\phi$. Other conventions are as in Fig. 9D. The inset shows a standing hexagonal array with the definition of the interommatidial angle, $\Delta\phi$. (B) Scanning electron micrograph showing the right eye of a male *Xenos vesparum* viewed from the side. Dorsal is at the top. Scale bar, 100 μm.

measured response curve (Fig. 9A). The results show that, for small values of $\Delta\phi=1°$ and $\Delta\phi=5°$ with $\Delta\rho=2\Delta\phi$, the rising part of the EMD response characteristic lies at short spatial wavelengths, far below the values at which the amplitude of the measured optomotor response rises (filled circles in Fig. 9A). Furthermore, with $\Delta\phi>1°$, the model output shows multiple sign reversals that are not evident in the experimental results. We next used the same values for $\Delta\phi$, but low-pass-filtered the output by assuming $\Delta\rho$ values that were 10 times

the size of $\Delta\phi$ (Fig. 9B). This set of variables shifts the maximum of the EMD output towards slightly longer wavelengths, produces a shallower slope of the characteristic and dampens the oscillations at short wavelengths. Fig. 9C demonstrates in more detail how variations in $\Delta\rho$ affect the overall response characteristic, specifically the sign reversals and the location of the maximum.

Up to this point, we can see that the model output comes closest to the experimental data with a sampling distance of approximately 10° and an angular acceptance function of 60° (Fig. 9C), in so far as the rising part of the model output curve and its maximum are located in the same range of spatial wavelengths as the measured optomotor response curve. The sign reversals at shorter wavelengths, however, still remain significant. The optomotor characteristic we measured does not show these inversions, although the predicted amplitudes are large enough to be detectable experimentally. In the case of $\Delta\phi$=10°, the inverted response amplitude amounts to approximately one-third of the response maximum (Fig. 9C).

Why did we fail to find a response inversion of the strepsipteran optomotor response? In the following, we would like to suggest two reasons for the absence of an inversion. First, EMDs with different sampling bases may contribute to the response. It is known from the analysis of the optomotor response and of motion-sensitive neurons in flies that motion detectors with different sampling bases can contribute significantly to motion sensitivity (Buchner, 1976, 1984; Pick and Buchner, 1979; Schuling et al., 1989). In *Drosophila melanogaster*, the sampling distance between the EMD input elements was found to correspond to the interommatidial angle and twice the interommatidial angle, such that the detector, with an input separation of $\Delta\phi$, contributes 70% to the total response (Buchner, 1976). Second, we have so far considered the output of a motion-detection network with equally spaced input elements. The ommatidia in strepsipteran eyes, however, are not arranged in regular rows, as is the case in the eyes, or parts of the eyes, of other insects (see Fig. 10B). It is possible, therefore, that the discrepancy between the experimental data and the model predictions is due to an irregular sampling array in the strepsipteran eye.

We tested whether the observed response could be a consequence of both multiple and irregularly spaced sampling bases by assuming sampling bases to be distributed normally with a maximum at 10° and $\Delta\rho$ to be 60°, as shown in Fig. 9C. We then calculated the model response by superimposing weighted contributions from sampling distances spaced one, two and three times the standard deviation from the principal component (Fig. 9D). The model output of such an irregularly spaced EMD array improves the fit to the relevant experimental data at short and medium wavelengths, with wider distributions being better. We systematically varied the variables and found the best fit as judged by the average-squared differences between the experimental data and the model response, for $\Delta\phi$ values between 8° and 10°, a distribution of sampling bases with a standard deviation of $0.5\Delta\phi$, and for $\Delta\rho$ values between 48° and 60° (Fig. 10A). Average-squared differences are 0.023 for 8±4° ($\Delta\rho$=48°), 0.017 for 9±4.5° ($\Delta\rho$=54°) and 0.021 for 10±5° ($\Delta\rho$=60°).

We are left with a considerable difference between the model output and the measured response data at long spatial wavelengths above 60° which, however, is not critical for our attempt to identify visual system variables. The comparatively large amplitudes of the measured response at long wavelengths may be a consequence of the particular patterns we used in our experiments. At large spatial wavelengths, the response to gratings with rectangular intensity profiles probably contains not only the main component elicited by the fundamental spatial wavelength λ but also fractions of responses to the third and higher harmonics of the stimulus pattern. For this reason, the response to gratings with low spatial frequencies contains a mixture of wavelength-dependencies that combine to increase responses in the motion detectors. We therefore feel justified in ignoring these data points for the comparison of the experimental data and the EMD model output, although we have included them in our measurement of goodness of fit.

Discussion

We have presented an experimental analysis of the optomotor response to investigate the spatial resolution of the compound eyes in male *X. vesparum*. The anatomical organisation of the eyes suggests two possibilities: the resolution could be limited by the angular separation between neighbouring ommatidia and, as a result, be rather low, or the insects could make use of the resolution potentially provided by individual receptor cells of the extended retinas behind each of the large facet lenses, a possibility suggested by anatomical data (Strohm, 1910; Rösch, 1913; Wachmann, 1972; Buschbeck et al., 1999). In the latter case, one would expect a much better resolution than that determined by the angular separation of the facets. The results of modelling the optomotor response characteristic that we measured in *X. vesparum* suggest that the sampling base, $\Delta\phi$, must lie close to 9° and that the width of the angular acceptance function of the input elements, $\Delta\rho$, must be unusually large, approximately 50°.

In assessing the significance of our data for answering the question we raised, we face the problem that the interommatidial angles in strepsipteran compound eyes are difficult to measure. *In vivo* optical measurements, which would be the method of choice, are not available, because the animals are extremely fragile and very short-lived. Anatomical measurements are hampered by the fact that the facet array is irregular, and it is difficult to find a plane for histological sections that would contain a row of neighbouring facets. Nevertheless, we estimated the interommatidial angle in semi-thin sections stained with Methylene Blue by selecting instances in which two neighbouring ommatidia were lying in one plane. We found an average value for $\Delta\phi$ of 19.2±4.2° (mean ± S.D., N=28). This value corresponds reasonably well with the 10–12 facets situated roughly at the eye equator in

scanning electron micrographs of *X. vesparum* heads when viewed from above, suggesting that horizontal interommatidial angles lie between 15° and 18°, assuming a horizontal visual field of approximately 180°. The anatomical estimates of $\Delta\phi$ are therefore approximately twice as large as the principal sampling base we identified by modelling the optomotor characteristic. This is what we would expect to find if motion detection takes place between neighbouring ommatidia in a standing hexagonal array (see inset in Fig. 10A) in which horizontal image motion stimulates neighbouring facets in vertically adjacent rows with an effective sampling base of half the interommatidial angle.

Since we could only model the experimental data by assuming that the sampling array in Strepsiptera is irregular, we also estimated the irregularities by measuring the distance from a particular lens to its six neighbours in scanning electron micrographs taken from a viewing direction perpendicular to the eye surface. In two animals, we found average values for the inter-facet distance of 41.3±4 μm (N=79) and 47.1±6.6 μm (N=59) (means ± S.D.). With a standard deviation in the range of 10% of the mean, sampling irregularities are quite significant (see also Fig. 10B).

The large $\Delta\rho$ value needed to model the optomotor response in *X. vesparum* is, in our opinion, the most relevant piece of evidence needed to solve the problem we posed at the beginning of this study. It is hard to see how such a large value of the angular acceptance function can be reconciled with the hypothesis that the elementary motion-detection process underlying the optomotor response in *X. vesparum* is based on interactions between individual receptor cells in each of the retinas. From light and electron microscopic sections of the eye, we judge the angle subtended by the retina at the nodal point of the lenses (which we assumed to lie at the centre of curvature of the lens) to be 53.9±13.4° (mean ± S.D., N=17), which is in good agreement with the range of values for $\Delta\rho$ determined in the behavioural experiments.

Both the behavioural resolution in the context of the optomotor response and the anatomical estimates show that functional resolution in strepsipteran compound eyes is limited by an interommatidial angle of approximately 18° and an angular sensitivity function of approximately 50°. We therefore find no evidence to support the hypothesis that the extended retina behind each lens in the strepsipteran compound eye provides the animals with better resolution than that given by the interommatidial angle. Let us add the caveat at this point that we arrive at our conclusions after having studied the optomotor response and, although there is no evidence for it, the possibility remains that *X. vesparum* males may use the potentially superior resolution of their unusual eyes for other visual behavioural tasks, such as object detection and obstacle avoidance.

There are, however, a number of further facts about the anatomy of the strepsipteran eye that make it unlikely that the eyes are designed to exploit the potential resolution of their extended retinas, as has recently been suggested (Buschbeck et al., 1999): (i) the rhabdomeres in the back focal plane of each lens are not optically isolated from each other by screening pigment (Wachmann, 1972; W. Pix, unpublished data); (ii) they are arranged in an intricate network in which the rhabdomeres of groups of retinula cells are closely coupled (Fig. 1D); (iii) the retinas of strepsipteran ommatidia are tiered (Wachmann, 1972; W. Pix, unpublished observations) so that the number of functional rhabdomeric units available for sampling at the back focal plane of each lens is much smaller than the number of receptors associated with each ommatidium; (iv) the transition from the originally night-active Strepsiptera to the derived day-active species is accompanied by an increase in facet numbers (Kinzelbach, 1967, 1971), indicating that the waning need for a high absolute light sensitivity and the increasing need for spatial resolution at high ambient light levels required more sampling stations at the level of the ommatidia, and not at the level of the retinal lattice; (v) a notable feature of strepsipteran compound eyes is the lack of regular packing of the ommatidia. This is true not only for the arrangement of facets within one eye, but also for the surprisingly variable numbers of facets in the right and the left eyes of the same individual (Kinzelbach, 1967, 1971). French et al. (1977) have pointed out that irregular sampling is equivalent to low-pass-filtering of the image. Strepsipteran eye design is not optimised in terms of spatial resolution.

Our behavioural results, taken together with the anatomical observations listed above, raise a number of generally relevant questions that are worth further investigation. An array of widely separated ommatidia, as is found in the visual system of strepsipteran males and in trilobites (Fordyce and Cronin, 1993; Horváth et al., 1997), would theoretically cause serious aliasing problems for the visual system over a wide range of spatial wavelengths. The irregularity of the ommatidial array in strepsipteran eyes (see also Kinzelbach, 1967, 1971) could be one way of attenuating the magnitude of response inversions generated by the lattice of elementary motion detectors. To understand how an animal copes with the reduced spatial information provided by such irregularly spaced input elements with large sampling distances and acceptance angles, it is necessary to learn more about the function of vision in male Strepsiptera. An interesting possibility is that eye design in Strepsiptera is driven solely by the constraints of estimating self-motion parameters from optic flow. Recent studies probing the principal limits of this task suggest that spatial resolution is the least important point in this context (Dahmen et al., 1997). In fact, robust self-motion estimates require optic flow measurements at only a few, but widely spaced, positions in the visual field, a conjecture that makes the sparsely sampling compound eyes of Strepsiptera in terms of the number of ommatidia appear like a very stripped-down, but efficient, visual self-motion sensor. Support for this comes from the observation that, in those strepsipteran species showing systematic variations in facet sizes across the eye, lens diameters tend to be larger in the ventral than in the dorsal part of the eye (Kinzelbach, 1971, part 1, 1990; Pohl and Melber, 1996).

It will be interesting to determine whether the eyes of strepsipteran males serve other visual functions apart from the control of self-motion. Tasks that come to mind, and for which a higher spatial resolution may be required, are host detection or obstacle avoidance during flight. Considering that few scientists have seen Strepsiptera alive, this will certainly not be an easy task. For the time being, however, the estimates of the functional variables of the strepsipteran eye, which we have determined in behavioural experiments, provide a strong motivation to carry out a detailed analysis of the anatomy of these peculiar eyes. Before filing them away under 'junk vision', we would, for instance, like to know how the tiered retinas are organised in detail, to what extent retinula cell axon projections from neighbouring ommatidia overlap at the level of the lamina and how this relates to the overlap of visual fields. An important additional point will be to determine accurately the scale of the rearrangement of retinula cell axons on their way to the lamina, the 'twist' in axon bundles that has been observed by Buschbeck et al. (1999). Since our results show that the visual fields of ommatidia are likely to overlap, the twist in the axon bundles may indicate convergence in the lamina of those axons from neighbouring ommatidia that carry information from the same region in space. There is growing evidence that, after all, the Strepsiptera are closely related to the Diptera (Kinzelbach, 1990; Whiting and Wheeler, 1994; Chalwatzis et al., 1995), and their eyes, which are unusual both in their functional characteristics and in their anatomical make-up, might turn out to be instructive informants about the origins of neural superposition eyes (Zeil, 1983; Nilsson and Ro, 1994; Land et al., 1999).

The study was in part financed by a DAAD postgraduate fellowship to W.P. All three of us are grateful for the opportunity to work at the Centre for Visual Sciences at the Australian National University and for the support we received from Mandyam Srinivasan. We thank Roland Hengstenberg and Dezsö Varjú for the loan of equipment, support and many fruitful discussions. This work and the manuscript benefited greatly from discussions with Hansjürgen Dahmen, Gerbera Nalbach, Gert Stange and Mandyam Srinivasan and from technical support by Heinz Bendele. We are grateful to Roger Heady, Horst Schoppmann and Sally Stowe for their help with the histological sections and the scanning electron micrographs.

References

Borst, A. and Egelhaaf, M. (1989). Principles of visual motion detection. *Trends Neurosci.* **12**, 297–306.

Borst, A. and Egelhaaf, M. (1993). Detecting visual motion: Theory and models. In *Visual Motion and its Role in the Stabilization Of Gaze* (ed. F. A. Miles and J. Wallman), pp. 3–27. Amsterdam, London: Elsevier.

Buchner, E. (1976). Elementary movement detectors in an insect visual system. *Biol. Cybernetics* **24**, 85–101.

Buchner, E. (1984). Behavioural analysis of spatial vision in insects. In *Photoreception and Vision in Invertebrates* (ed. M. A. Ali), pp. 561–621. New York, London: Plenum Press.

Buschbeck, E., Ehmer, B. and Hoy, R. (1999). Chunk *versus* point sampling: Visual imaging in a small insect. *Science* **286**, 1178–1180.

Chalwatzis, N., Baur, A., Stetzer, E., Kinzelbach, R. and Zimmermann, F. K. (1995). Strongly expanded 18S rRNA genes correlated with a peculiar morphology in the insect order of Strepsiptera. *Zoology* **98**, 115–126.

Crowson, R. A. (1981). *The Biology of Coleoptera*. London, New York, Toronto: Academic Press.

Dahmen, H. J., Wüst, R. M. and Zeil, J. (1997). Extracting egomotion parameters from optic flow: Principal limits for animals and machines. In *From Living Eyes to Seeing Machines* (ed. S. Venkatesh and M. V. Srinivasan), pp. 174–198. Oxford: Oxford University Press.

Fordyce, D. and Cronin, T. W. (1993). Trilobite vision: a comparison of schizochroal and holochroal eyes with the compound eyes of modern arthropods. *Paleobiol.* **19**, 288–303.

French, A. S., Snyder, A. W. and Stavenga, D. G. (1977). Image degradation by an irregular retinal mosaic. *Biol. Cybernetics* **27**, 229–233.

Götz, K. G. (1964). Optomotorische Untersuchungen des visuellen Systems einiger Augenmutanten der Fruchtfliege *Drosophila*. *Kybernetik* **2**, 77–92.

Götz, K. G. (1965). Die optischen Übertragungseigenschaften der Komplexaugen von *Drosophila*. *Kybernetik* **2**, 215–221.

Götz, K. G., Hengstenberg, B. and Biesinger, R. (1979). Optomotor control of wing beat and body posture in *Drosophila*. *Biol. Cybernetics* **35**, 101–112.

Hassenstein, B. (1951). Ommatidienraster und afferente Bewegungsintegration. *Z. Vergl. Physiol.* **33**, 301–326.

Hengstenberg, R. (1993). Multisensory control in insect oculomotor systems. In *Visual Motion and its Role in the Stabilization of Gaze* (ed. F. A. Miles and J. Wallmann), pp. 285–298. Amsterdam, London: Elsevier.

Horváth, G., Clarkson, E. N. K. and Pix, W. (1997) Survey of modern counterparts of schizochroal Trilobite eyes: Structural and functional similarities and differences. *Historical Biol.* **12**, 229–263.

Jancke, G. D. (1955). Zur Morphologie der männlichen Cocciden. *Z. Angew. Ent.* **37**, 265–314.

Kathirithamby, J. (1989). Review of the order Strepsiptera. *Syst. Ent. Lond*. **14**, 41–92.

Kinzelbach, R. (1967). Zur Kopfmorphologie der Fächerflügler (Strepsiptera, Insecta). *Zool. Jb. Anat.* **84**, 559–684.

Kinzelbach, R. (1971). Morphologische Befunde an Fächerflüglern und ihre phylogenetische Bedeutung (Insecta: Strepsiptera). *Zoologica* **41** (119, parts 1 and 2), 1–256.

Kinzelbach, R. (1990). The systematic position of Strepsiptera (Insecta). *Am. Ent.* **36**, 292–303.

Land, M. F. (1997). Visual acuity in insects. *Annu. Rev. Ent.* **42**, 147–177.

Land, M. F., Gibson, G., Horwood, J. and Zeil, J. (1999). Fundamental differences in the optical structure of the eyes of nocturnal and diurnal mosquitoes. *J. Comp. Physiol.* A **185**, 91–103.

Linsley, E. G. and MacSwain, J. W. (1957). Observations on the habits of *Stylops pacifica* Bohart (Coleoptera: Stylopidae). *Univ. Calif. Publ. Ent.* **11**, 395–430.

Nilsson, D.-E. and Ro, A.-I. (1994). Did neural pooling for night

vision lead to the evolution of neural superposition eyes? *J. Comp. Physiol.* A **175**, 289–392.

Paulus, H. F. (1979). Eye structure and the monophyly of the Arthropoda. In *Arthropod Phylogeny* (ed. A. P. Gupta), pp. 299–383. New York: Van Nostrand Reinhold.

Pick, B. and Buchner, E. (1979). Visual movement detection under light- and dark-adaptation in the fly, *Musca domestica*. *J. Comp. Physiol.* **134**, 45–54.

Pix, W., Nalbach, G. and Zeil, J. (1993). Strepsipteran forewings are haltere-like organs of equilibrium. *Naturwissenschaften* **80**, 371–374.

Pohl, H. and Melber, A. (1996). Verzeichnis der mitteleuropäischen Fächerflügler und die Beschreibung einer neuen Art der Gattung *Malayaxenos* Kifune 1981 (Insecta: Strepsiptera). *Senckenbergiana Biol.* **75**, 171–180.

Reichardt, W. (1987). Evaluation of optical motion information by movement detectors. *J. Comp. Physiol.* A **161**, 533–547.

Rösch, P. (1913). Beiträge zur Kenntnis der Entwicklungsgeschichte der Strepsiptera. *Jena Z. Naturw.* **50** (N.F. 43), 97–146.

Schuling, F. H., Mastebroek, H. A. K., Bult, R. and Lenting, B. P. M. (1989). Properties of elementary movement detectors in the fly *Calliphora erythrocephala*. *J. Comp. Physiol.* A **165**, 179–192.

Shannon, C. E. and Weaver, W. (1949). *The Mathematical Theory of Communication*. Urbana: University of Illinois Press.

Strohm, K. (1910). Die zusammengesetzten Augen der Männchen von *Xenos rossi*. *Zool. Anz.* **36**, 156–159.

Ulrich, W. (1956). Unsere Strepsipteren-Arbeiten. *Zool. Beitr.* **N.F. 2**, 177–255.

von Gavel, L. (1939). Die ‘kritische Streifenbreite’ als Maß der Sehschärfe bei *Drosophila melanogaster*. *Z. Vergl. Physiol.* **27**, 80–135.

Wachmann, E. (1972). Zum Feinbau des Komplexauges von *Stylops* spec. (Insecta, Strepsiptera). *Z. Zellforsch.* **123**, 411–424.

Warrant, E. J. and McIntyre, P. D. (1993). Arthropod eye design and the physical limits to spatial resolving power. *Progr. Neurobiol.* **40**, 413–461.

Whiting, M. F. and Wheeler, W. C. (1994). Insect homeotic transformation. *Nature* **368**, 696.

Zanker, J. M. (1988). How does lateral abdomen deflection contribute to flight control of *Drosophila melanogaster*? *J. Comp. Physiol.* A **162**, 581–588.

Zeil, J. (1983). Sexual dimorphism in the visual system of flies: The compound eyes and neural superposition in Bibionidae (Diptera). *J. Comp. Physiol.* A **150**, 379–393.